11th International Symposium on Turbulence and Shear Flow Phenomena (TSFP11)
Southampton, UK, July 30 to August 2, 2019

# REYNOLDS NUMBER EFFECT OF TURBULENT DISSIPATION RATE IN A FULLY-DEVELOPED CHANNEL FLOW

**Yoshinobu Yamamoto**

Department of Mechanical Engineering...
University of Yamanashi
4-3-11, Takeda, Kofu 400-8511, Japan
yamamotoy@yamanashi.ac.jp

**Yoshiyuki Tsuji**

Department of Energy Science and Engineering.
Nagoya University
Furo Chikusa, Nagoya 464-8601, Japan
c42406a@nucc.cc.nagoya-u.ac.jp

## ABSTRACT

In this study, we have established the full-DNS database for fully developed turbulent channel flows up to fiction Reynolds number ($Re_\tau$) 8000. Aiming to investigate Reynolds number effects on turbulent dissipation-rate, grid-sensitivity analysis is carefully conducted. As the result the reliable data for not only mean velocity and turbulent intensities but also budgets of turbulent kinetic energy and dissipation rate are systematically obtained by means of a hybrid Fourier-spectral and second-order accurate finite difference DNS code.

Reynolds number effects on the distribution of the pre-multiplied dissipation rate are observed not only in the viscous sub-layer but also in the log-layer. This logarithmic region played the main role of Reynolds number effects on the dissipation-rate as same in turbulent kinetic energy. Therefore, local equilibrium between turbulent production and dissipation rate can be expected at the log-region with high-Re limits. Reynolds number effects on dissipation rate at the log-region can be also considered as the asymptotic behaviour toward the isotopic turbulence. However, in this range up to $Re_\tau$ =8000, the magnitude of the pre-multiplied dissipation rate is underestimated compared with the production of the turbulent kinetic energy. Consequently, the overproduction of turbulent kinetic energy is maintained at the log-layer.

## INTRODUCTION

To understand the Reynolds number effects on wall-bounded flows associated with large scale structures is very important form the viewpoints of the turbulent control and modelling in high Reynolds number conditions. One of the typical high-Reynolds number effects is the increasing of the inner-scaled peak in the streamwise turbulent intensity (DeGraff & Eaton, 2000, Metzger & Klewicki, 2001). On the other hand, the turbulent dissipation rate (ε) is also one of the characteristic parameters of turbulence. Abe & Antonia (2016) are investigated the relationship between the energy dissipation and the skin friction by means of DNS database up to $Re_\tau$ =5200 (Lee & Moser, 2015), where $Re_\tau$ is the friction Reynolds number based on the friction velocity ($u_\tau$) at the wall and the channel-half width ($h$) and showed that the logarithmic dependence of bulk mean velocity is clarified through the scaling behaviour of the turbulent energy dissipation rate. However, in the high-Reynolds number limits, the von Kármán constant (κ) between the streamwise mean velocity ($U$) and the turbulent dissipation rate can be expected to same with each other but they are different; κ =0.384 of $U$ and 0.408 of ε.

In this study, we focus on the Reynolds number effects of the turbulent dissipation rate and its tranport process by means of our new DNS database up to $Re_\tau$ =8000.

## DNS DATABASE

The reported target flow is assumed to be a fully developed turbulent channel flow driven by the constant mean pressure gradient in the streamwise direction as shown in Fig.1, where $h$ denotes the channel-half height, $x_1$=(=$x$), $x_2$(=$y$), and $x_3$(=$z$) is the streamwise, wall-normal, and spanwise directions, respectively. In this study, turbulent velocities are denoted as $u_1$(=$u$), $u_2$(=$v$), and $u_3$=($w$), respectively, with the mean velocity indicated by a capital letter.

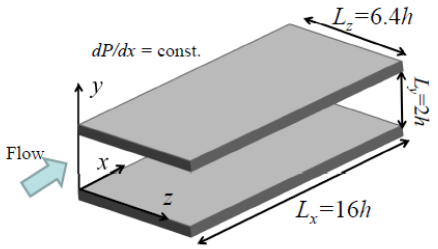


FIG.1. Computational domain and coordinate system.

TABLE 1. DNS conditions.

| $Re_\tau$ | $\Delta x^+$ | $\Delta y^+$ | $\Delta z^+$ | $T^+/Re_\tau$ | $U_b^+$ |
|---|---|---|---|---|---|
| 125 | 15.6 | 0.3-4.0 | 6.3 | 20.0 | 14.98 |
| 250 | 15.6 | 0.3-4.0 | 8.3 | 18.0 | 16.36 |
| 500 | 16.0 | 0.4-5.3 | 8.3 | 13.1 | 18.14 |
| 1000 | 16.0 | 0.6-8.0 | 8.3 | 12.0 | 19.92 |
| 2000 | 16.0 | 0.6-8.0 | 8.3 | 10.0 | 21.74 |
| 4000 | 16.0 | 0.6-8.0 | 8.3 | 8.0 | 23.27 |
| 8000 | 18.5 | 0.6-8.0 | 8.9 | 6.3 | 24.97 |

DNSs of the incompressible Navier-Stokes equation are performed by a hybrid Fourier-spectral for stream- and spanwise directions and second-order accurate finite-difference method for the wall-normal directions (Yamamoto & Kunugi, 2011, 2015). Aliasing errors for wall-parallel directions are removed by 3/2 rules. Initial conditions are used velocity fields of previous DNS database (Yamamoto & Tsuji, 2018).

The DNS conditions are summarized in Table 1, where $T$ denotes the time-integration length to obtain the turbulent statistics, $U_b$ denotes bulk mean velocity, and superscript + denotes the nondimensional quantity normalized by friction velocity ($u_\tau$) and kinematic viscosity (ν). $\Delta x$, $\Delta y$, $\Delta z$ are the grid resolutions for the streamwise, wall-normal, and spanwise directions, respectively. The range present DNS database of $Re_\tau$ is from 125 to 8000. The logarithmic profile in streamwise mean velocity ($U^+$) at $300 < y^+ < 1000$ ($y/h$=0.14) is confirmed in case of $Re_\tau$ =8000 with κ =0.387, where, $y$ is the distance from the wall

The turbulent kinetic energy ($k$) and the dissipation rate ($\varepsilon$) are defined as follow:

$$k = \frac{1}{2}\overline{u_i u_i}, \varepsilon = \nu\overline{\left(\frac{\partial u_i}{\partial x_j}\right)^2}. \quad (1)$$

Here, overbar — denotes the averaged value, and Einstein summation convention is adapted for an index variable appears twice in a single term.

The equations of $k$- and $\varepsilon$-budget are written as (Mansour, Kim, & Moin, 1988)

$$\frac{Dk}{Dt} = 0 = P_k + T_k + D_k + \Pi_k - \varepsilon, \quad (2)$$

$$\frac{D\varepsilon}{Dt} = 0 = P_\varepsilon^1 + P_\varepsilon^2 + P_\varepsilon^3 + P_\varepsilon^4 + T_\varepsilon + D_\varepsilon + \Pi_\varepsilon - \gamma. \quad (3)$$

The transport equation (2) of the turbulent kinetic energy is classified into three terms for types of their contributions; the production term ($P_k$), the diffusion terms comprised of the turbulent diffusion ($T_k$), the viscous diffusion ($D_k$) and the pressure diffusion ($\Pi_k$), and the dissipation term ($\varepsilon$ ).

The transport equation (3) of the turbulent energy dissipation rate is also classified into three terms. The production terms comprise the mixed production ($P_\varepsilon^1$), the production by mean velocity ($P_\varepsilon^2$), the gradient production ($P_\varepsilon^3$), and the turbulent production ($P_\varepsilon^4$). The diffusion terms comprise the turbulent diffusion ($T_\varepsilon$), the pressure diffusion ($\Pi_\varepsilon$), and the viscous diffusion ($D_\varepsilon$). The destruction (dissipation) terms comprise the viscous destruction rate ($\gamma$). The definition of these terms is summarized in Appendix A.

In the log-layer of $U$, the premultiplied turbulent kinetic energy production ($y^+P_k^+$) in a fully-developed channel flow is estimated as

$$y^+P_k^+ = \left(1 - \frac{y^+}{\mathrm{Re}_\tau} - \frac{1}{\kappa y^+}\right)\frac{1}{\kappa}. \quad (4)$$

In the limit $\mathrm{Re}_\tau \to \infty$, $y^+P_k^+$ shows the value: $1/\kappa$ at the log-later ( $y^+ > 100$). With the assumption of the equilibrium between $P_k$ and $\varepsilon$: $P_k \sim \varepsilon$, $y^+\varepsilon^+$ also shows the value: $1/\kappa$.

## VALIDATION OF PRESENT DNS DATABASE

TABLE 1. DNS conditions for $\mathrm{Re}_\tau$ =1000.

| CASE | $L_x/h$ ($N_x$) | $L_y/h$ ($N_x$) | $L_z/h$ ($N_x$) | $\Delta x^+$ | $\Delta y^+$ | $\Delta z^+$ |
|---|---|---|---|---|---|---|
| C | 16 (864) | 2 (512) | 6.4 (720) | 18.5 | 0.6-8.0 | 8.9 |
| N | 16 (1000) | 2 (512) | 6.4 (768) | 16.0 | 0.6-8.0 | 8.3 |
| H | 16 (2000) | 2 (512) | 6.4 (1000) | 8.0 | 0.6-8.0 | 6.4 |
| LM | $8\pi$ (2304) | 2 (512) | $3\pi$ (2048) | 10.9 | 0.02-6.2 | 6.2 |

The adequacy of the grid resolution used for the present DNSs has been verified through a grid sensitivity study at $\mathrm{Re}_\tau$ =1000, for reasons of computational feasibility. Wall-parallel grid resolutions are gradually changed with wall-normal resolution is constant because twice finer resolution is adapted compared to the Kolmogorov wave number in the wall-normal direction. Numerical conditions for this grid sensitivity study in case of $\mathrm{Re}_\tau$ =1000 are summarized in TABLE 2, here CASE C is as same resolution in case of $\mathrm{Re}_\tau$=8000, CASE N is as same resolution in cases between $\mathrm{Re}_\tau$=125 and 4000, and LM is the high-resolution DNS database of Lee & Moser (2015).

Figure 2 (a) shows the streamwise turbulent intensity profiles near wall-region. The peaks of the streamwise turbulent intensity in CASE C and N are slightly underestimated with comparison of LM.

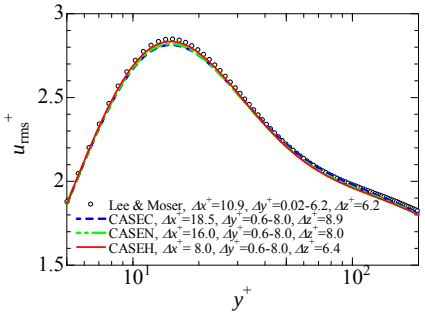


(a) Streamwise turbulent intensity

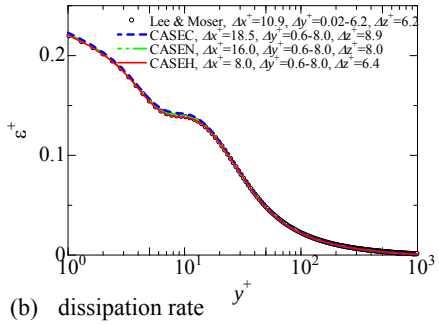


(b) dissipation rate

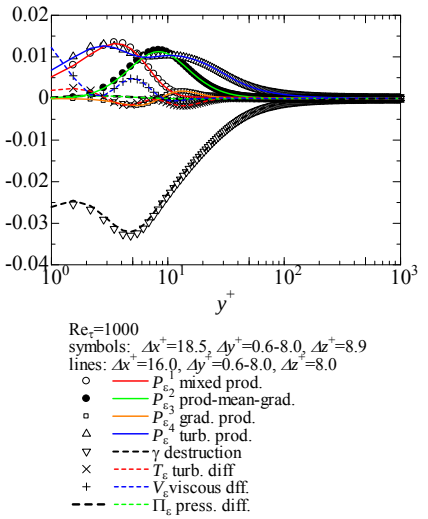


(c) Budget of dissipation rate

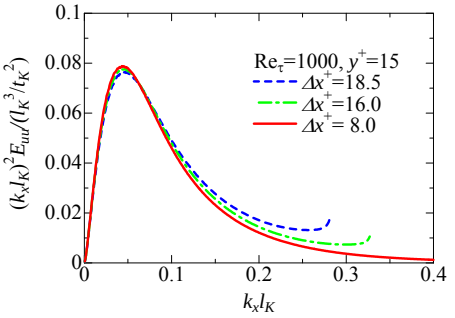


(d) Streamwise dissipation spectra at $y^+$=15.

FIG 2 grid resolution effects on streamwise turbulent intensity and turbulent dissipation rate in case of $\mathrm{Re}_\tau$ =1000.

Figure 2 (b)-(d) shows the grid resolution effects on turbulent dissipation rate. Both of profiles and budget for dissipation rate correspond reasonably well, regardless of differences of grid resolution. This is caused the grid resolution even in CACE C can be resolved the peak of dissipation spectra as shown in Fig.2 (d). Therefore, we conclude that present DNS database can be applied for investigation of dissipation rate with the enough accuracy.

## RESULTS AND DISSCUSSIONS

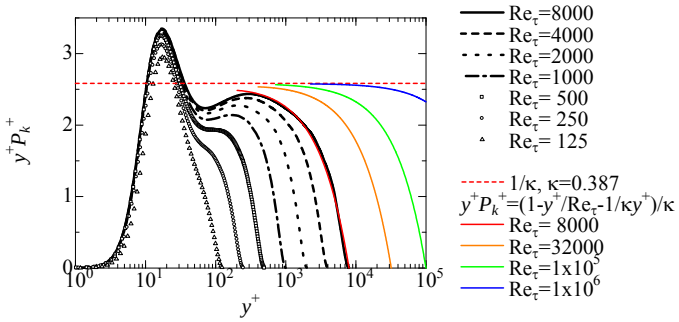


FIG 3 Premultiplied turbulent production ($y^+P_k^+$).

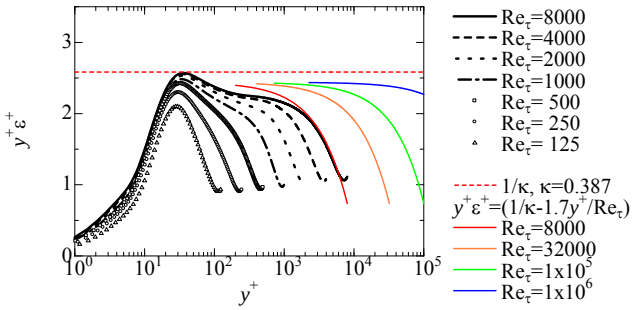


FIG 4 Premultiplied dissipation rate ($y^+\varepsilon^+$).

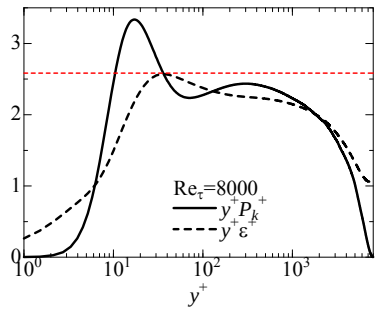


FIG 5 Comparison of premultiplied-turbulent production and -dissipation rate.

### Profiles of turbulent production and dissipation rate

Figure 3 shows the Re-dependency of the pre-multiplied turbulent kinetic energy production. With increasing of $Re_\tau$, the value of $y^+P_k^+$ at the logarithmic region increases but it's value dose not reach 2.58(=1/κ, κ=0.387 at $Re_\tau$=8000). Because the value of $Re_\tau$=8000 is in good agreement with one of eq. (4), $y^+P_k^+$ will reach the 2.58 at $Re_\tau$ =32000.

Figure 4 also shows the Re-dependency of the pre-multiplied turbulent dissipation rate, where color-lines are fitting equation; $y^+\varepsilon^+$ =2.45-1.7$y$/$h$ by Abe & Antonia (2016). Reynolds number effects are observed both in the viscous layer and log-layer. The peak values of $y^+\varepsilon^+$ show the almost 2.58 (=1/κ, κ=0.387) at $y^+$~40, but underestimate at the log-layer.

Compared with $y^+P_k^+$, $y^+\varepsilon^+$ shows the slowly increasing tendency, as the results the overproduction of $k$ is maintained at the log-layer as shown in Fig.5.

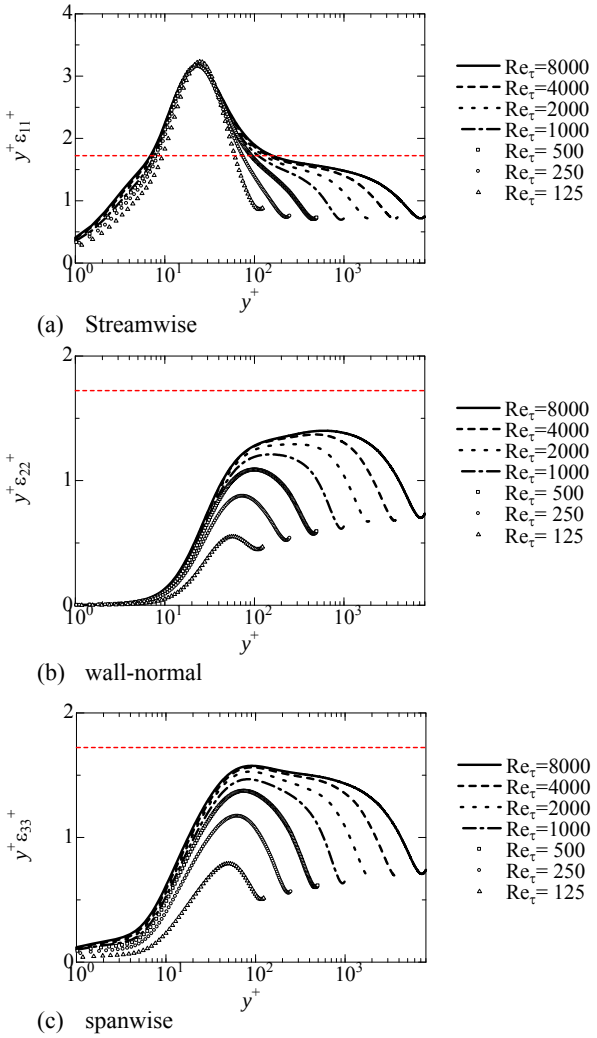


FIG 6 Premultiplied dissipation rate ($y^+\varepsilon_{ii}^+$).

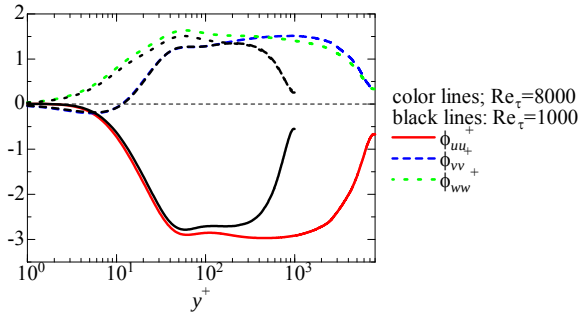


FIG 7 Premultiplied pressure-strain ($y^+\phi_{ii}^+$).

Figure 6 shows Re-dependency of $y^+\varepsilon_{ii}^+$. Streamwise dissipation ($\varepsilon_{11}$) has the remarkable peak at $y^+$~30, but this peak value is independent of $Re_\tau$ as shown in Fig.6 (a). The only wall-normal dissipation rate ($\varepsilon_{22}$) has the double peaks for $Re_\tau$ > 2000 as shown in Fig. 6 (b). In Fig. 6 (c), spanwise dissipation rate ($\varepsilon_{33}$) has the most similar profile with total dissipation rate ($\varepsilon$) at the log-region. Accordingly, increasing

tendency of ε at log-region is mainly caused from the wall-normal dissipation rate ($\varepsilon_{22}$). In fact, the wall-normal pressure-strain term ($\phi_{22}$) exceeds the spanwise pressure-strain term ($\phi_{33}$) from log-region to outer layer in $Re_\tau > 4000$ as shown in Fig.7.

**Budget of turbulent dissipation rate**

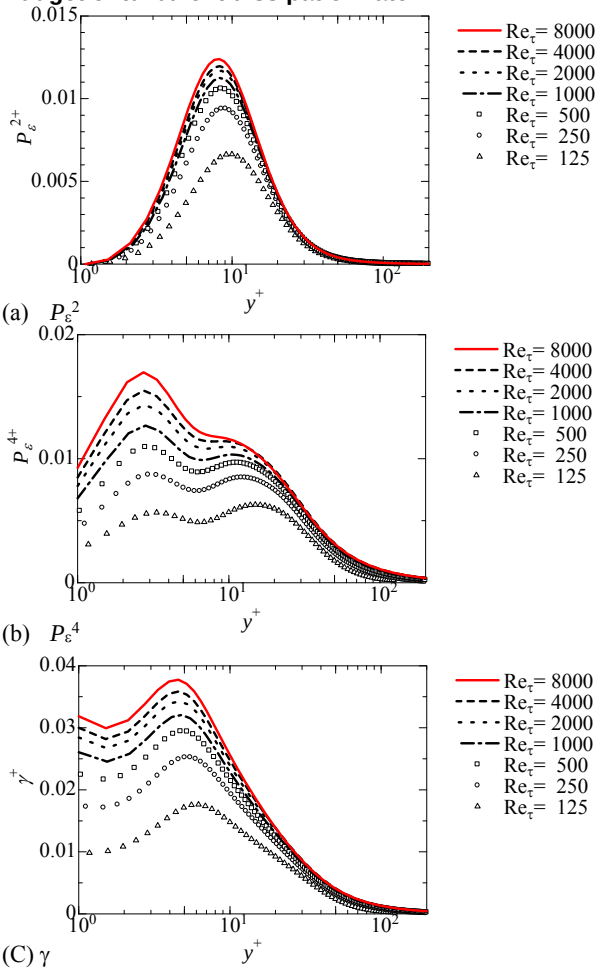


FIG.8 Re-dependency of ε-budget.

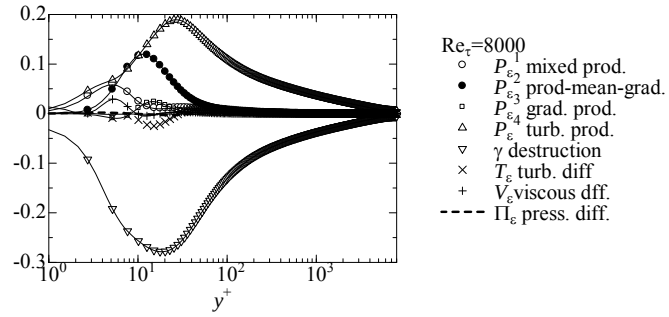


FIG. 9 Premultiplied ε-budget

Figure 8 shows the Reynolds number dependency of terms in ε-budget in Eq.(3). Rodi & Mansour (1993) argued the scaling of the terms in ε-budget, and estimated that the terms of $P_\varepsilon^1$ and $P_\varepsilon^2$decreased, the terms of $P_\varepsilon^4$ and γ increase as Re increases. In Fig.8 (a), the term of $P_\varepsilon^2$ slightly increases with increasing of $Re_\tau$. This is caused from the dependency of mean shear rate ($S=dU/dy$). On the other hands, the terms of $P_\varepsilon^4$ and γ increase with increasing of $Re_\tau$ as shown in Figs. 8(b) and (c). Eventually, $P_\varepsilon^4$ exceeds $P_\varepsilon^1$over all wall-normal height in $Re_\tau > 4000$ as suggestion by Rodi & Mansour (1993).

Figure 9 shows the premultiplied ε-budget in $Re_\tau$=8000. Turbulent production ($yP_\varepsilon^4$) has the largest peak at $y^+$~30. This wall-normal height is corresponded to the peak location of $y\varepsilon$ as shown in Fig. 4. On the other hands, destruction ($y\gamma$) has the peak value at more the wall-side: $y^+$~20.

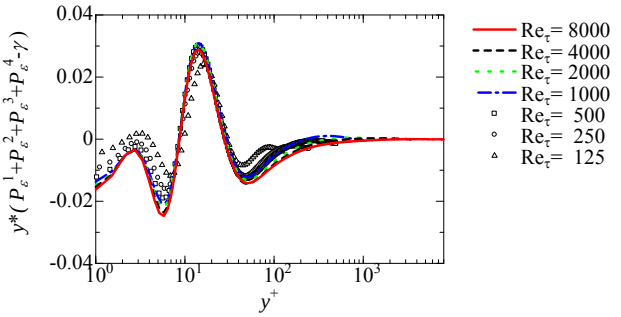


FIG. 10 Premultiplied of production – destruction in ε-budget

Figure 10 shows the premultiplied of $P_\varepsilon^1$+ $P_\varepsilon^2$+ $P_\varepsilon^3$+ $P_\varepsilon^4$–γ in ε-budget in Eq. (3). In $Re_\tau$=8000, the local equilibrium between production and destruction in ε-budget is completed from the log-region to the outer-layer. The negative peak is observed at the wall-normal height; $y^+$~40. This wall-normal height is corresponded to the valley profile of $y\varepsilon$ as shown in Fig. 4.

**Balance of integral turbulent production and dissipation rate over the channel cross section**

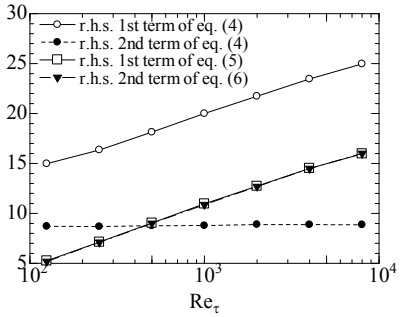


FIG 11 integral energy balance over the channel cross section

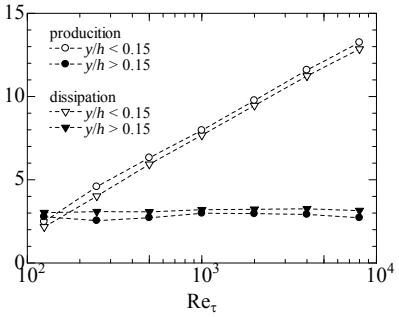


FIG.12 contribution integral values of turbulent production ($P_k$) and dissipation rate at inner-layer ($y/h< 0.15$) and outer-layer ($y/h>0.15$).

In a fully-developed channel flow, the integral over the channel cross section of $P_k$ can be estimated by the variation of the bulk velocity ($U_b$) and one of the turbulent dissipation rate

(ε). In channel flow, $P_k$ has the following relationships with $U_b$ and ε:

$$0 = U_b^+ - \int_0^{h^+} \left( \frac{dU^+}{dy^+} \right)^2 dy^+ + \int_0^{h^+} \overline{u^+v^+} \frac{dU^+}{dy^+} dy^+ \quad , \tag{4}$$

$$0 = \int_0^{h^+} -\overline{u^+v^+} \frac{dU^+}{dy^+} dy^+ - \int_0^{h^+} \varepsilon^+ dy^+ \quad . \tag{5}$$

Figure 11 shows the Reynolds number effects on Eqs.(4) and (5). Bulk mean velocity is logarithmically increased with increasing of $Re_\tau$. The second term of the right-hand side in Eq. (4) is the integral value of the mean energy dissipation rate, and it's value is almost constant (=9.13) as pointed out by Abe & Antonita (2016). The integral values of turbulent production ($P_k$) and dissipation rate (ε) are completely balanced according to Eq.(5). In this Re-range up to $Re_\tau$=8000, turbulent production

Figure 12 shows the contribution integral values of turbulent production and dissipation rate at the inner-layer ($y/h < 0.15$) and outer-layer ($y/h > 0.15$). The inner-layer takes main part in energy increasing. On the other hands, the contribution of the outer-layer is almost constant in both terms. From eq.(4), in the limit $Re_\tau \to \infty$, $y^+P_k^+$ shows the value: 1/κ. In fact, $y^+P_k^+$ might shows 0.98/κ in $Re_\tau \approx O(10^5)$, as shown in Fig.3. Therefore, logarithmically Re-effects on the inner-layer as shown in Fig.12 must be achieved by not increasing of local peaks of $y^+P_k^+$ but the spread of the logarithmic region. This is also same in premultiplied dissipation rate. These results might indicate that mismatch between production and dissipation rate at the log-region as shown in Fig.4 is decreased at the extreme high Reynolds number.

## Local equilibrium between turbulent production and dissipation rate

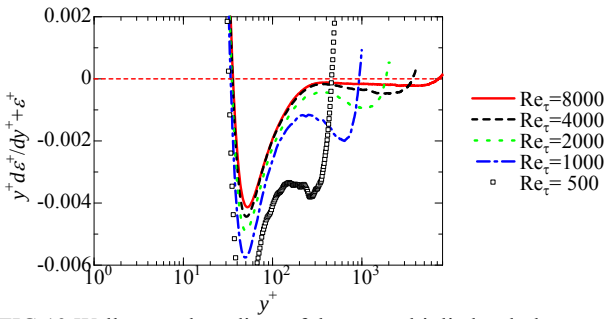


FIG 13 Wall-normal gradient of the premultiplied turbulent dissipation rate.

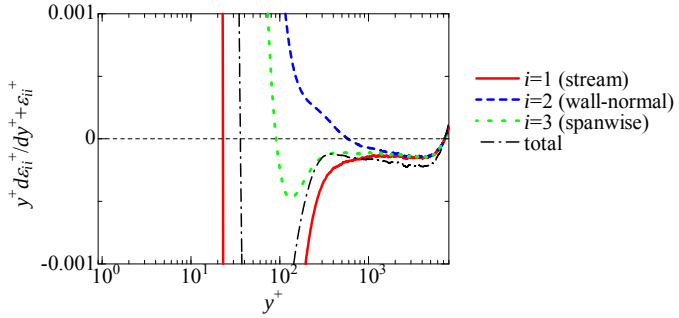


FIG 14 Wall-normal gradient of the premultiplied turbulent dissipation rate for stream, wall-normal and spanwise direction in $Re_\tau$=8000.

Figure 13 shows the wall-normal gradient of $y^+\varepsilon^+$. All cases show the minus values at $y^+ > 100$.With the assumption of the equilibrium between $P_k$ and ε, the wall-normal gradient of $y^+\varepsilon^+$ shows zero at the log-layer in the limit $Re_\tau \to \infty$. In case of $Re_\tau$=8000, the value of $d(y^+\varepsilon^+)/dy^+$ asymptotes to zero at the log-layer. However, the value of $y^+\varepsilon^+$ in case of $Re_\tau$ =8000 underestimates 2.58 (=1/κ). Thereby $d(y^+\varepsilon^+)/dy^+$ once needs to have the positive value and tends to zero at the log-later in cases of $Re_\tau >> 8000$. In $Re_\tau$=8000, this increasing tendency of the wall-normal gradient toward the local equilibrium can be only observed in wall-normal dissipation rate ($\varepsilon_{22}$) as shown in Fig.14.

Figure 15 shows the premultiplied dissipation rate for stream, wall-normal, and spanwise directions in $Re_\tau$ =1000 and 8000. At the log-region, all components underestimate the high-Re limit value: 2/(3κ). Particularly, spanwise component is less than 2/(3κ) in the all wall-normal height. Therefore, it is suggested that the wall-normal gradient of spanwise dissipation rate ($\varepsilon_{33}$) will be change to positive at higher Re than $Re_\tau$ =8000. Furthermore, these results also indicates that all components show the same value: 2/(3κ) at the log-region. In other words, isotropic behaviours will be promoted with increasing of $Re_\tau$, and local equilibrium between turbulent production and dissipation rate at the log-region is just the isotropic status of the dissipation rate.

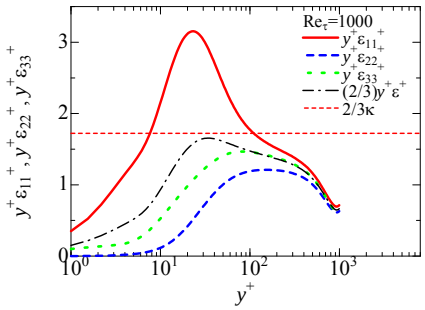


(a) $Re_\tau$=1000

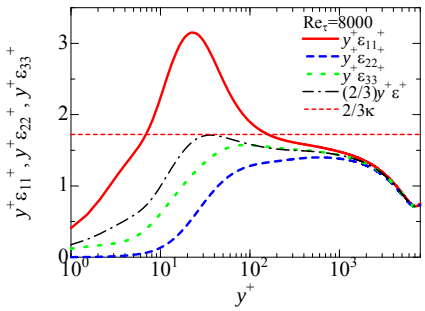


(b) $Re_\tau$=8000

FIG.15 premultiplied dissipation rate for stream, wall-normal, and spanwise direction.

## CONCLUSION

Reynolds number effects of turbulent dissipation rate ( ε ) and its transport process in a fully-developed channel have been investigated by means of the DNS database up to friction Reynolds number 8000. Near wall region, the scaling arguments of the terms in the ε-equation by Rodi & Mansour (1993) are completed for the present Reynolds numbers; the turbulent production ($P_\varepsilon^4$) and destruction (γ) terms are clearly depended on Reynolds number and the balance between $P_\varepsilon^4$ and γ are confirmed from the log-layer to the channel centre. Reynolds number effects on the distribution of the pre-multiplied dissipation rate are observed not only in the viscous

sub-layer but also in the log-layer. In the log-layer, the dissipation rate shows the tendency of isotropic behaviours with increasing of $Re_\tau$. In the high-Re limits, local equilibrium between turbulent production and dissipation rate at the log-region will be expected. This equilibrium status is just the isotropic status of the dissipation rate. However, in the present Re- range up to $Re_\tau$ =8000, the magnitude of the pre-multiplied dissipation rate is underestimated compared with the production of the turbulent kinetic energy ($k$). Consequently, the overproduction of $k$ is maintained at the log-layer.

## APPENDIX A

The budgets of turbulent kinetic energy and dissipation rate are express as follows:

$$\frac{D\overline{uu}}{Dt} = \underbrace{-2\overline{uv}\frac{\partial U}{\partial y}}_{P_{11}} + \underbrace{\frac{\partial}{\partial y}\left(-\overline{uuv}\right)}_{T_{11}} + \underbrace{2\overline{\frac{p}{\rho}\frac{\partial u}{\partial x}}}_{\phi_{11}} + \underbrace{\frac{\partial}{\partial y}\left(\nu\frac{\partial \overline{uu}}{\partial y}\right)}_{V_{11}} \underbrace{-2\nu\overline{\left(\frac{\partial u}{\partial x_j}\right)^2}}_{\varepsilon_{11}} = 0 \tag{A-1}$$

$$\frac{D\overline{vv}}{Dt} = \underbrace{\frac{\partial}{\partial y}\left(-\overline{vvv}\right)}_{T_{22}} + \underbrace{2\frac{\partial}{\partial y}\left(-\frac{\overline{pv}}{\rho}\right)}_{\Pi_{22}} + \underbrace{2\overline{\frac{p}{\rho}\frac{\partial v}{\partial y}}}_{\phi_{22}} + \underbrace{\frac{\partial}{\partial y}\left(\nu\frac{\partial \overline{vv}}{\partial y}\right)}_{V_{22}} \underbrace{-2\nu\overline{\left(\frac{\partial u}{\partial x_j}\right)^2}}_{\varepsilon_{22}} = 0 \tag{A-2}$$

$$\frac{D\overline{ww}}{Dt} = \underbrace{\frac{\partial}{\partial y}\left(-\overline{wwv}\right)}_{T_{33}} + \underbrace{2\overline{\frac{p}{\rho}\frac{\partial w}{\partial z}}}_{\phi_{33}} + \underbrace{\frac{\partial}{\partial y}\left(\nu\frac{\partial \overline{ww}}{\partial y}\right)}_{V_{33}} \underbrace{-2\nu\overline{\left(\frac{\partial w}{\partial x_j}\right)^2}}_{\varepsilon_{33}} = 0 \tag{A-3}$$

$$\frac{Dk}{Dt} = \underbrace{\frac{P_{11}}{2}}_{P_k} + \underbrace{\frac{T_{11}+T_{22}+T_{33}}{2}}_{T_k} + \underbrace{\frac{\Pi_{22}}{2}}_{\Pi_k} + \underbrace{\frac{V_{11}+V_{22}+V_{33}}{2}}_{V_k} \underbrace{-\frac{\varepsilon_{11}+\varepsilon_{22}+\varepsilon_{33}}{2}}_{\varepsilon} = 0 \tag{A-4}$$

$$\begin{aligned}\frac{D\varepsilon}{Dt} = & \underbrace{-2\nu\overline{\frac{\partial u}{\partial x_i}\frac{\partial v}{\partial x_i}}\frac{\partial U}{\partial y}}_{P_\varepsilon^1} \underbrace{-2\nu\overline{\frac{\partial u_i}{\partial x}\frac{\partial u_i}{\partial y}}\frac{\partial U}{\partial y}}_{P_\varepsilon^2} \underbrace{-2\nu\nu\overline{\frac{\partial u}{\partial y}}\frac{\partial^2 U}{\partial y^2}}_{P_\varepsilon^3} \underbrace{-2\nu\overline{\frac{\partial u_i}{\partial x_j}\frac{\partial u_i}{\partial x_k}\frac{\partial u_k}{\partial x_j}}}_{P_\varepsilon^4} \\ & + \underbrace{\frac{\partial}{\partial y}\left(-\nu\overline{\frac{\partial u_i}{\partial x_j}\frac{\partial u_i}{\partial x_j}}\nu\right)}_{T_\varepsilon} + \underbrace{\frac{\partial}{\partial y}\left(-2\nu\overline{\frac{1}{\rho}\frac{\partial p}{\partial x_i}\frac{\partial v}{\partial x_i}}\right)}_{\Pi_\varepsilon} \\ & + \underbrace{\nu\frac{\partial^2\varepsilon}{\partial y^2}}_{D_\varepsilon} \underbrace{-2\nu^2\overline{\frac{\partial^2 u_i}{\partial x_j\partial x_k}\frac{\partial^2 u_i}{\partial x_j\partial x_k}}}_{\gamma} = 0\end{aligned} \tag{A-5}$$

## ACKNOLODGEMENT

This research used computational resources of NEC SX-ACE provided by Japan Agency for Marin-Earth Science and Technology (JAMSTEC) through the HPCI System Research project (Project ID: hp190108).

## REFERENCES

Abe, H., & Antonia, R. A. (2016). Relationship between the energy dissipation function and the skin friction law in a turbulent channel flow. *J. Fluid Mech., 798*, 140-164.

DeGraff, D., & Eaton, J. (2000). Reynolds-number scaling of the flat-plate turbulent boundary layer. *J. Fluid Mech., 422*, 319-346.

Lee, M., & Moser, R. D. (2015). Direct numerical simulation of turbulent channel flow up to Reτ = 5200. *J. Fluid Mech., 774*, 395-415.

Mansour, M. N. Kim, J, & Moin, P. (1988). Reynolds-stress and dissipation-rate budgets in a turbulent channel flow. *J. Fluid Mech., 194*, 15-44.

Metzger, M. M., & Klewicki, J. C. (2001). A comparative study of near-wall turbulence in high and low Reynolds number boundary layers. *Phys. Fluids, 13*(3), 692-701.

Yamamoto, Y., & Kunugi, T. (2011). Direct numerical simulation of a high-Froude-number turbulent open-channel flow. Physics of Fluids, 23(12), 125108.

Yamamoto, Y., & Kunugi, T. (2016). MHD effects on turbulent dissipation process in channel flows with an imposed wall-normal magnetic field. Fusion Engineering and Design, 109, 1137-1142.

Yamamoto, Y., & Tsuji, Y. (2018). Numerical evidence of logarithmic regions in channel flow at Reτ = 8000. *Phys. Rev. Fluids, 3*, 012602(R).

Rodi, W., & Mansour, N. N. (1993). Low Reynolds number k—ε modelling with the aid of direct simulation data. Journal of Fluid Mechanics, 250, 509-529.